

The Effect of Mass Ratio and Air Damper Characteristics on the Resonant Response of an Air Damped Dynamic Vibration Absorber

Ranjit G. Todkar¹, Shridhar G. Joshi²

¹ Department of Mechanical Engineering, P.V.P. Institute of Technology, Budhagaon, Sangli, India

² Department of Mechanical Engineering, Walchand College of Engineering, Sangli, India

E-mail: rgtodkar@gmail.com

Received October 21, 2011; revised November 25, 2011; accepted November 12, 2011

Abstract

In this paper, it is shown that, a road vehicle 2DOF air damped quarter-car suspension system can conveniently be transformed into a 2DOF air damped vibrating system representing an air damped dynamic vibration absorber (DVA) with an appropriate change in the ratio μ of the main mass and the absorber mass *i.e.* when mass ratio $\mu \gg 1$. Also the effect of variation of the mass ratio, air damping ratio and air spring rate ratio, on the motion transmissibility at the resonant frequency of the main mass of the DVA has been discussed. It is shown that, as the air damping ratio in the absorber system increases, there is a substantial decrease in the motion transmissibility of the main mass system where the air damper has been modeled as a Maxwell type. Optimal value of the air damping ratio for the minimum motion transmissibility of the main mass of the system has been determined. An experimental setup has been designed and developed with a control system to vary air pressure in the damper in the absorber system. The motion transmissibility characteristics of the main mass system have been obtained, and the optimal value of the air damping ratio has been determined for minimum motion transmissibility of the main mass of the system

Keywords: Air Damped Dynamic Vibration Absorber, Motion Transmissibility, Effect of Mass Ratio, Air Damper, Optimization

1. Introduction

Many real engineering systems such as, a road vehicle suspension system, a dynamic vibration absorber system, a vibration isolation system of machinery (where the floor supporting the machine is sufficiently flexible), a double centrifugal pendulum system etc., can be adequately represented as 2DOF vibrating systems [1]. As such, in this paper, a 2DOF air damped vibrating system representing a 2DOF air damped dynamic vibration absorber has been studied. In this case, the mass ratio μ *i.e.*, ratio of the main mass m_2 to the auxiliary mass m_1 is greater than unity ($\mu \gg 1$) and is in the range of 2.5 to 5.0. Also the effect of variation of the mass ratio, air spring rate ratio and air damping ratio on the motion transmissibility of main mass has been discussed. It has been shown that, as the air damping ratio in the absorber system increases, there is a substantial decrease in the motion transmissibility of the main mass system in the neighborhood of

resonant frequency for the case where the air damper is modeled as a Maxwell type [2,3]. Optimal value of the air damping ratio for the minimum transmissibility of the main mass system has been determined. An experimental setup has been designed with an air pressure control system for setting the appropriate value of air damping ratio in the system. The motion transmissibility characteristics of the main mass m_2 of the dynamic vibration absorber model have been obtained.

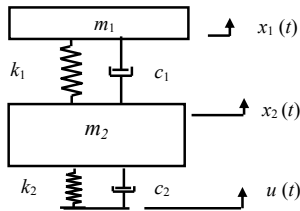
2. Equations of Motion

Equations of motion have been derived and are given respectively in **Tables 1, 2** and **3** for the following [2],

1) A 2DOF dynamic vibration absorber system with system damping only and without air damper (Refer **Figure 1** in **Table 1**), here after referred as Case 1.

2) A 2DOF air damped dynamic vibration absorber system with system damping and, Vogit type model for

Table 1. A general 2DOF viscously damped vibrating system with system damping.



A general 2DOF vibrating system (Dynamic Vibration Absorber Model). $\mu \gg 1$.

Equations of motion

$$m_2 \ddot{x}_2 = -k_1(x_2 - x_1) - c_1(\dot{x}_2 - \dot{x}_1) - k_2(x_2 - u) - c_2(\dot{x}_2 - \dot{u}) \quad (1)$$

$$m_1 \ddot{x}_1 = -k_1(x_1 - x_2) - c_1(\dot{x}_1 - \dot{x}_2) \quad (2)$$

$$Mt2 = \frac{X_2}{U} = \left[\frac{[-A_{22}\lambda^2 + A_{00}]^2 + [A_{11}\lambda]^2}{[B_4\lambda^4 - B_2\lambda^2 + B_0]^2 + [-B_3\lambda^3 + B_1\lambda]^2} \right]^{\frac{1}{2}} \quad (3)$$

$$Mt1 = \frac{X_1}{U} = \left[\frac{[-A_2\lambda^2 + A_0]^2 + [A_1\lambda]^2}{[B_4\lambda^4 - B_2\lambda^2 + B_0]^2 + [-B_3\lambda^3 + B_1\lambda]^2} \right]^{\frac{1}{2}} \quad (4)$$

where

$$A_{22} = 2\zeta_2, A_{11} = v^2 + 4\zeta_1\zeta_2v, A_{00} = 2(\zeta_1v^2 + \zeta_2v), \text{ and}$$

$$A_2 = 4\zeta_1\zeta_2v, A_1 = 2\zeta_1v^2, A_0 = v^2 \text{ and}$$

$$B_4 = 1, B_3 = 2(\zeta_1 + (\zeta_1/\mu) + \zeta_2v), B_2 = (1 + (1/\mu) + v^2),$$

$$B_1 = 2(v\zeta_2 + \zeta_1v^2), B_0 = v^2$$

air damper (Refer **Figure 2** in **Table 2**), hereafter referred as Case 2.

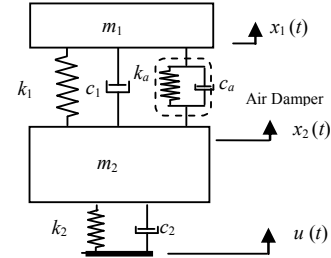
3) A 2DOF air damped dynamic vibration absorber system with system damping and with Maxwell type model for air damper (Refer **Figure 3** in **Table 3**), hereafter referred as Case 3.

Motion Transmissibility

Assuming the steady state solutions in the form $x_1 = X_1 e^{j\omega t}$, $x_2 = X_2 e^{j\omega t}$ and $y = Y e^{j\omega t}$ the base excitation as $u = U e^{j\omega t}$ and following the usual procedure of solution, the equations of motion have been solved and the expressions for the motion transmissibility Mt2 (for the main mass) and Mt1 (for the auxiliary mass) have been obtained and are given respectively in Equations (3) and (4) for Case 1 in **Table 1** and in Equations (7) and (8) for Case 2 in **Table 2** and in Equations (12) and (13) in **Table 3**. [4].

Table 2. 2DOF Air damped vibrating system using an air damper (Vigot Model), with system damping coefficients c_1 , c_2 and air damper characteristics i) air damping. Ratio ζ_a and ii) air spring rate ratio $k = (k_a/k_1)$, where k_1 = stiffness of auxiliary spring and k_a = stiffness of air spring.

Case 2



DOF air damped vibrating system using an air damper (Vigot Model). (Dynamic Vibration Absorber Model). $\mu \gg 1$.

Equations of motion

$$m_2 \ddot{x}_2 = -(k_1 + k_a)(x_2 - x_1) - (c_1 + c_a)(\dot{x}_2 - \dot{x}_1) - k_2(x_2 - u) - c_2(\dot{x}_2 - \dot{u}) \quad (5)$$

$$m_1 \ddot{x}_1 = -(k_1 + k_a)(x_1 - x_2) - (c_1 + c_a)(\dot{x}_1 - \dot{x}_2) \quad (6)$$

$$Mt2 = \frac{X_2}{U} = \left[\frac{[-a_{22}\lambda^2 + a_{00}]^2 + [a_{11}\lambda]^2}{[b_4\lambda^4 - b_2\lambda^2 + b_0]^2 + [-b_3\lambda^3 + b_1\lambda]^2} \right]^{\frac{1}{2}} \quad (7)$$

$$Mt1 = \frac{X_1}{U} = \left[\frac{[-a_2\lambda^2 + a_0]^2 + [a_1\lambda]^2}{[b_4\lambda^4 - b_2\lambda^2 + b_0]^2 + [-b_3\lambda^3 + b_1\lambda]^2} \right]^{\frac{1}{2}} \quad (8)$$

where

$$a_{22} = 2\zeta_2v,$$

$$a_{11} = (v^2 + 4\zeta_1\zeta_2v + 4\zeta_a k^{0.5}\zeta_2v),$$

$$a_{00} = 2(\zeta_1v^2 + \zeta_a k^{0.5}v^2 + \zeta_2v + k\zeta_2v)$$

and

$$a_2 = 4\zeta_1\zeta_2v + 4\zeta_2\zeta_a k^{0.5}v$$

$$a_1 = 2(\zeta_1v^2 + \zeta_a k^{0.5}v^2 + \zeta_2v + k\zeta_2v)$$

$$a_0 = 2(\zeta_1v^2 + \zeta_a k^{0.5}v^2 + \zeta_2v + k\zeta_2v),$$

$$a_0 = v^2(1 + k)$$

and

$$b_4 = 1, b_3 = 2(\zeta_1 + (\zeta_1/\mu) + \zeta_2v + \zeta_a[k^{0.5} + (k^{0.5}/\mu)])$$

$$b_2 = (1 + k + 4\zeta_1v\zeta_2 + 4\zeta_a k^{0.5}v\zeta_2 + (1/\mu) + v^2 + (k/\mu))$$

$$b_1 = 2(v\zeta_2 + k v \zeta_2 + \zeta_1v^2 + \zeta_a k^{0.5}v^2),$$

$$b_0 = v^2(1 + k)$$

Table 3. 2DOF air damped vibrating system using an air damper (Maxwell Model), with system damping coefficients c_1, c_2 and air damper characteristics air damping ratio ζ_a and air spring ratio $k = (k_a/k_1)$, where $k_1 =$ stiffness of auxiliary spring and $k_a =$ stiffness of air spring.

	<p>Equations of motion</p> $m_2 \ddot{x}_2 = -k_1(x_2 - x_1) - c_1(\dot{x}_2 - \dot{x}_1) - k_a(x_2 - y) - k_2(x_2 - u) - c_2(\dot{x}_2 - \dot{u}) \quad (9)$ $-c_a(\dot{y} - \dot{x}_1) - k_a(y - x_2) = 0 \quad (10)$ $m_1 \ddot{x}_1 = -k_1(x_1 - x_2) - c_1(\dot{x}_1 - \dot{x}_2) - c_a(\dot{x}_1 - \dot{y}) \quad (11)$ $Mt2 = \frac{X_2}{U} = \left[\frac{[a_{44}\lambda^4 - a_{22}\lambda^2 + a_{00}]^2 + [a_{35}\lambda^3 - a_{33}\lambda^3 + a_{11}\lambda]^2}{[-b_6\lambda^6 + b_1\lambda^4 - b_2\lambda^2 + b_0]^2 + [b_3\lambda^5 - b_3\lambda^3 + b_1\lambda]^2} \right]^{\frac{1}{2}} \quad (12)$ $Mt1 = \frac{X_1}{U} = \left[\frac{[a_4\lambda^4 - a_2\lambda^2 + a_0]^2 + [-a_3\lambda^3 + a_1\lambda]^2}{[-b_6\lambda^6 + b_1\lambda^4 - b_2\lambda^2 + b_0]^2 + [b_3\lambda^5 - b_3\lambda^3 + b_1\lambda]^2} \right]^{\frac{1}{2}} \quad (13)$
--	---

2DOF Air damped vibrating system using an air damper (Maxwell Model) $\mu \gg 1$. dynamic vibration absorber model.

where

$$\delta = k^{0.5}/(2 \zeta_a)$$

$$a_{55} = 2 \zeta^2 v, a_{44} = [v^2 + 4 \delta \zeta_2 v + 4 \zeta_1 \zeta_2 v], a_{33} = [2\delta v^2 + 8 \delta \zeta_1 \zeta_2 v + 2\zeta_1 v^2 + 2v \delta (\zeta_1 + \zeta_2) + \zeta_2 v (1+2k)]$$

$$a_{22} = [\delta^2 v (v + 4 \zeta_1 \zeta_2) + \delta v (4 \zeta_1 v + 4 \zeta_2 + 2 \zeta_2 k) + v^2(I + k)], a_{11} = \delta^2 (4 \zeta_1 v^2 + 2 \zeta_2 v) + \delta(k v^2 + 2 v^2), a_{00} = \delta^2 v^2$$

and

$$a_4 = 4 \zeta_1 \zeta_2 v, a_3 = 2\zeta_1 v^2 + 8 \delta \zeta_1 \zeta_2 v + 2 \zeta_2 v(I + k),$$

$$a_2 = \delta[4\zeta_1 v^2 + 2 \zeta_2 v + k 2 \zeta_2 v + 2 \zeta_2 v] + 4\delta \zeta_1 \zeta_2 v + v^2[1 + k],$$

$$a_1 = \delta^2 2 v [\zeta_1 v + \zeta_2] + \delta v^2 [2 + k], a_0 = \delta^2 v^2$$

and

$$b_6 = 1, b_5 = (2 \delta + 2 \zeta_1 + (2 \zeta_1/\mu) + 2 \zeta_2 v), b_4 = [1 + k + (1/\mu) + v_2 + (k/\mu) + 4 \zeta_1 \zeta_2 v] + 4 \delta [\zeta_1 + (\zeta_1/\mu) + \zeta_2 v] + \delta_2$$

$$b_3 = \delta[2 + 8 \zeta_1 \zeta_2 v + (2/\mu) + 2 v^2 + k + (k/\mu)] + [2 \zeta_2 v + 2 \zeta_2 v k + 4 \zeta_1 \zeta_2 v^2] + \delta_2 [2 \zeta_1 + (2 \zeta_1/\mu) + 2 \zeta_2 v],$$

$$b_2 = \delta^2 [1 + 4 \zeta_1 \zeta_2 v + (1/\mu) + v^2] + \delta [4 \zeta_2 v + 4 v^2 \zeta_1 + 2 \zeta_2 v k] + v^2(1+k), b_1 = \delta^2 [2 \zeta_2 v + 4 v^2 \zeta_1] + 2 \delta v^2,$$

$$b_0 = \delta^2 v^2$$

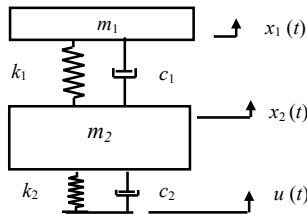


Figure 1. A general 2DOF vibrating system (dynamic vibration absorber model). $\mu \gg 1$.

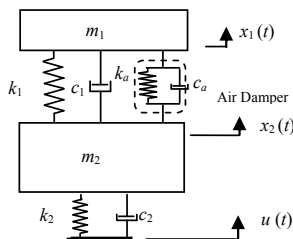


Figure 2. 2DOF air damped vibrating system using an air damper (vigot model). (dynamic vibration absorber model). $\mu \gg 1$.

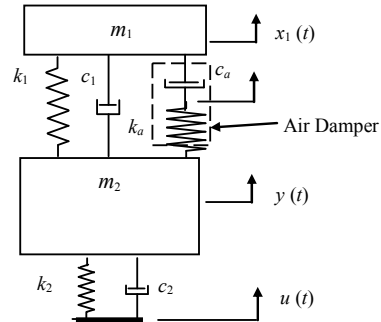


Figure 3. 2DOF air damped vibrating system using an air damper (maxwell model) $\mu \gg 1$. dynamic vibration absorber model.

3. Motion Transmissibility Mt2 ($\mu \gg 1$)

For the air damped dynamic vibration absorber system, mass ratio μ has been varied in the range of 2.5 to 5.0, where λ is the ratio of excitation frequency w to the undamped natural frequency w_1 of the system (m_1, k_1), have

been plotted for Case 1, Case 2 and Case 3. The peak values of Mt2 (at resonance) are given in **Tables 4, 5 and 6** respectively.

3.1. Effect of Variation of Mass Ratio μ

The values of μ are varied as $\mu = 2.5$, $\mu = 3.3$ and $\mu = 5.0$ when $\zeta_1 = 0.1$, $\zeta_2 = 0$, $k = 0.1$ and $\zeta_a = 0.05$ with spring

rate ratio (k_2/k_1) as 6.49. **Table 4** gives respectively the peak values of Mt2 at resonant frequencies obtained for Case 1, Case 2 and Case 3. It is seen that, as the value of μ increases, there is no substantial change in the value of Mt2 at the first resonant frequencies for the case where the air damper is modeled as a Maxwell type. **Figure 4, Figure 5 and Figure 6** show the corresponding Mt2 vs λ plots.

Table 4. Peak values of Mt2 with $\zeta_1 = 0.100$, $\zeta_2 = 0.0$, $k = 0.1$ and $\zeta_a = 0.05$ and value of mass ratio μ is varied.

Peak Values of Mt2		$\mu = 2.5$			$\mu = 3.3$			$\mu = 5.0$		
		With system damping only Case 1	Air damper modeled as a		With system damping only Case 1	Air damper modeled as a		With system damping only Case 1	Air damper modeled as a	
			Vigot Model Case 2	Maxwell Model Case 3		Vigot Model Case 2	Maxwell Model Case 3		Vigot Model Case 2	Maxwell Model Case 3
1st peak	Mt2	10.032	2.5732	0.487	7.652	2.3208	0.61	18.63	6.008	0.4948
	λ	0.91	0.920	1.01	0.91	0.92	1.0	0.87	0.88	1.01
2nd Peak	Mt2	4.295	7.42	4.3402	3.4503	5.8782	5.154	6.662	4.1069	1.428
	λ	1.76	1.79	1.64	1.76	1.78	1.64	1.3	1.35	1.35

Table 5. Peak values of Mt2 with $\mu=3.3$, $\zeta_1=0.133$, $\zeta_2=0.0$ and $\zeta_a = 0.05$ and value of spring rate ratio k is varied.

Peak Values of Mt2		$k = 0.075$			$k = 0.100$			$k = 0.150$		
		With system damping only Case 1	Air damper modeled as a		With system damping only Case 1	Air damper modeled as a		With system damping only Case 1	Air damper modeled as a	
			Vigot Model Case 2	Maxwell Model Case 3		Vigot Model Case 2	Maxwell Model Case 3		Vigot Model Case 2	Maxwell Model Case 3
1st peak	Mt2	9.2	2.836	0.5698	9.2	2.90	0.6152	9.2	3.045	0.6872
	λ	0.90	0.91	1.00	0.90	0.91	1.00	0.90	0.93	1.01
2nd peak	Mt2	4.357	5.244	2.535	4.357	5.09	2.87	4.357	3.49	4.81
	λ	1.53	1.57	1.48	1.53	1.57	1.49	1.53	1.51	1.59

Table 6. Peak values of Mt2 with $\mu = 3.3$, $\zeta_1 = 0.133$, $\zeta_2 = 0.0$ and $k = 0.10$ and value of air damping ratio ζ_a is varied.

Peak Values of Mt2		$\zeta_a = 0.025$			$\zeta_a = 0.05$			$\zeta_a = 0.075$		
		With system damping only Case 1	Air damper modeled as a		With system damping only Case 1	Air damper modeled as a		With system damping only Case 1	Air damper modeled as a	
			Vigot Model Case 2	Maxwell Model Case 3		Vigot Model Case 2	Maxwell Model Case 3		Vigot Model Case 2	Maxwell Model Case 3
1st peak	Mt2	9.2	3.077	0.8848	9.2	2.9	0.6152	9.2	2.752	0.5135
	λ	0.9	0.91	1.02	0.9	0.91	1.00	0.9	0.915	0.99
2nd peak	Mt2	4.357	5.157	7.367	4.357	5.090	2.87	4.357	5.035	2.011
	λ	1.53	1.58	1.53	1.53	1.57	1.49	1.53	1.57	1.47

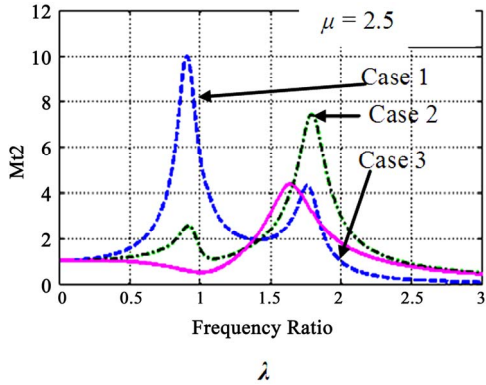


Figure 4. Mt2 vs λ when $\zeta_1 = 0.1, \zeta_2 = 0, k = 0.1$ and $\zeta_a = 0.05$.

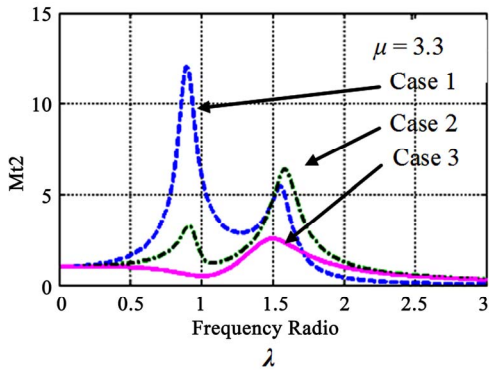


Figure 5. Mt2 vs λ when $\zeta_1 = 0.1, \zeta_2 = 0, k = 0.1$ and $\zeta_a = 0.05$.

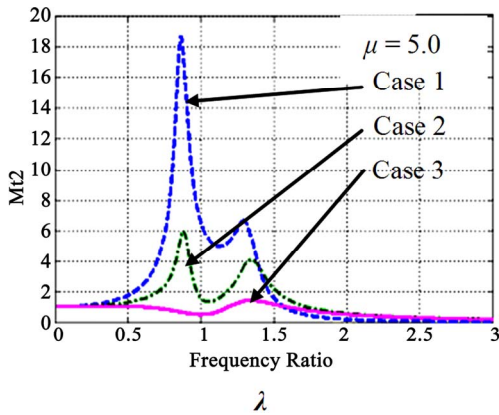


Figure 6. Mt2 vs λ when $\zeta_1 = 0.1, \zeta_2 = 0, k = 0.1$ and $\zeta_a = 0.05$.

3.2. Effect of Variation of Air Damper Spring Rate Ratio k

The values of k are varied as $k = 0.075, k = 0.10$ and $k = 0.15$ when $\zeta_1 = 0.133, \zeta_2 = 0.0, \mu = 3.3$ and $\zeta_a = 0.05$ with spring rate ratio (k_2/k_1) as 6.49. **Table 5** gives respectively the peak values of Mt2 at resonant frequencies obtained for Case 1, Case 2 and Case 3. It is seen that, as the value of air damper spring rate ratio k increases, there is a small increase in the peak value of Mt2 at the resonant

frequencies for the case where the air damper is modeled as a Maxwell type.

3.3. Effect of Variation of Air Damping Ratio ζ_a

The values of air damping ratio ζ_a are varied as $\zeta_a = 0.025, \zeta_a = 0.050$ and $\zeta_a = 0.075$ when $\mu = 3.3, \zeta_1 = 0.133, \zeta_2 = 0$ and $k = 0.10$ with spring rate ratio (k_2/k_1) as 6.49. **Table 6** gives respectively the peak values of Mt2 at resonant frequencies obtained for Case 1, Case 2 and Case 3. It is seen that, as the value of air damping ratio ζ_a increases there is a substantial decrease in the value of Mt2 at the resonant frequencies in the case where the air damper is modeled as a Maxwell type.

4. Optimal Value ζ_{aopt} of Air Damping Ratio ζ_a

The air damping is highly effective when the air damper was modeled as Maxwell type (Case 3). As such, a 2DOF air damped dynamic vibration absorber system for Case 3 is taken for optimization of air damping ratio ζ_a . The equation of the motion transmissibility Mt2 (of the main mass m2) is given by Equation (13) of **Table 3** for Case 3 when the air damper is modeled as a Maxwell type model [3]. The value of Mt2 is affected by the system parameters *i.e.* mass ratio μ , system damping ratio ζ_1 and the air damper characteristics 1) air spring rate ratio k and 2) air damping ratio ζ_a .

For minimizing the value of Mt2, consider equation (13) for Mt2 is

$$Mt2 = \frac{X_2}{U} = \sqrt{\frac{[a_{44}\lambda^4 - a_{22}\lambda^2 + a_{00}]^2 + [a_{55}\lambda^5 - a_{33}\lambda^3 + a_{11}\lambda]^2}{[-b_6\lambda^6 + b_4\lambda^4 - b_2\lambda^2 + b_0]^2 + [b_5\lambda^5 - b_3\lambda^3 + b_1\lambda]^2}} \quad (14)$$

(where constants $a_{44}, a_{33}, a_{22}, a_{11}, a_{00}, b_6, b_5, b_4, b_3, b_2, b_1$ and b_0 have been given in **Table 3**). The equation for Mt2 is rearranged in terms of ascending powers of ζ_a as

$$Mt2 = \frac{X_2}{U} = \sqrt{\frac{(A_4)\zeta_a^4 + (A_3)\zeta_a^3 + (A_2)\zeta_a^2 + (A_1)\zeta_a + (A_0)}{(B_4)\zeta_a^4 + (B_3)\zeta_a^3 + (B_2)\zeta_a^2 + (B_1)\zeta_a + (B_0)}} \quad (14)$$

where $A_4, A_3, A_2, A_1, A_0, B_4, B_3, B_2, B_1$ and B_0 are the constants containing system damping ratios $\zeta_1, \zeta_2, k, \mu, \lambda$ and v . The equation (14) for Mt2 is differentiated w.r.t. ζ_a and set equal to zero *i.e.* $\partial(Mt2)/\partial(\zeta_a) = 0$, a polynomial in terms of ζ_a is obtained as

$$h7\zeta_a^7 + h6\zeta_a^6 + h5\zeta_a^5 + h4\zeta_a^4 + h3\zeta_a^3 + h2\zeta_a^2 + h1\zeta_a + h0 = 0 \quad (15)$$

where h_i s ($i = 0, 1, 2, 3, 4, 5, 6$ and 7) are the constant coefficients containing μ, ζ_1, ζ_2, k and λ . The expressions derived for this are very lengthy and have not been included in the body of the write-up. The optimal value ζ_{aopt} of ζ_a is obtained by solving the Equation (15) and with the optimal value thus obtained the values of Mt2 have been determined.

4.1. Effect on Optimal ζ_{aopt} and on Mt2 for Various Values of Air Spring Rate Ratio k

The values of ζ_{aopt} for the air damper modeled as a Maxwell type model have been obtained for

- 1) $k = 0.025, k = 0.05, k = 0.075$ and $k = 0.1$ and the results are given in **Table 7**,
- 2) $k = 0.200, k = 0.3, k = 0.4$ and $k = 0.5$, the results are given in **Table 8** and
- 3) $k = 0.75, k = 1, k = 2$ and $k = 3$, the results are given in **Table 9** (Refer also **Figure 7**).

4.2. Effect of Air Spring Rate Ratio k on Optimal Value ζ_{aopt} of ζ_a When $\mu = 0.335, \zeta_1 = 0.133, \zeta_2 = 0.0$ and $\lambda = 1$

Figure 7 shows the effect k on Optimal Value ζ_{aopt} of air damping ratio ζ_a . From the results of analysis, it is seen that, as the value of ζ_{aopt} increases with the increase in air spring rate ratio k , the value of Mt2 increases. **Figure 7** shows the variation of the value of Mt2 with ζ_{aopt} for increasing values of k .

4.3. Effect of Variation of Mass Ratio μ on Optimal Value ζ_{aopt} of ζ_a

Figure 8 shows the effect of variation of mass ratio μ on ζ_{aopt} where air damper is modeled as a Maxwell type. The value of μ is varied as $\mu = 2.5$ and $\mu = 5.0$ when $\zeta_1 = 0.133, \zeta_2 = 0, k = 1$ and $\lambda = 1$ with the spring ratio (k_2/k_1)

Table 7. Values of ζ_{aopt} when air spring rate ratio k is varied.

Air Damper modeled as:	$\mu = 3.3, \zeta_1 = 0.133, \zeta_2 = 0.0, \lambda = 1$			
	$k = 0.025$	$k = 0.05$	$k = 0.075$	$k = 0.1$
Mt2 (min)	0.3804	0.3907	0.4004	0.4101
ζ_{aopt}	0.07	0.10	0.12	0.13

Table 8. Values of ζ_{aopt} when air spring rate ratio k is varied.

Air Damper modeled as:	$\mu = 3.3, \zeta_1 = 0.133, \zeta_2 = 0.0, \lambda = 1$			
	$k = 0.2$	$k = 0.3$	$k = 0.4$	$k = 0.5$
Mt2 (min)	0.4452	0.4754	0.5014	0.5236
ζ_{aopt}	0.18	0.21	0.23	0.24

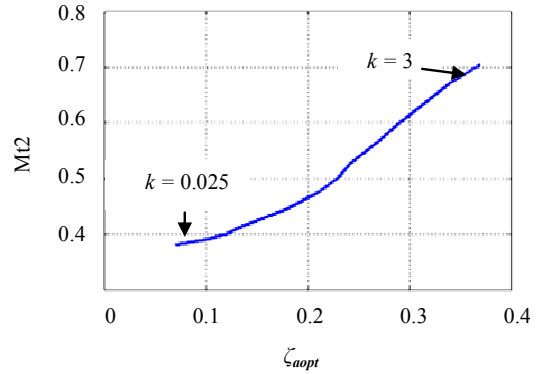


Figure 7. Mt2 vs ζ_a (Effect of k) for $k = 0.025$ to 3.0 .

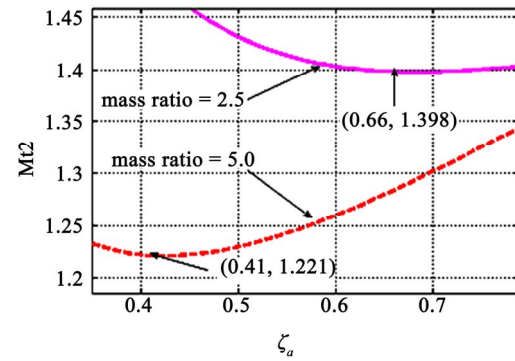


Figure 8. Mt2 vs ζ_a (Effect of μ).

as 6.49. It is seen that, as the value of μ increases, there is a significant reduction in the value of ζ_{aopt} and there is also a substantial decrease in the minimum value of Mt2.

5. Experimental Setup

Figure 9 shows the experimental setup designed and developed for dynamic response analysis of the 2DOF air damped dynamic vibration absorber system (refer also **Plate 1**). The setup consists of a cam operated mechanism to provide sinusoidal base excitation. The necessary software has been developed to collect and process the dynamic displacements to obtain graphical plots of the input excitation $u(t)$ vs time and the main mass response motion $x_2(t)$ vs time. The system also incorporates the facility to control the operating air pressure in the system through a computer interfaced system as shown in **Figure 9**. The values of the main mass and auxiliary mass have been selected in accordance with values reported in the literature. The ratio of main mass m_2 to auxiliary m_1 is about 5 to 10. The 2DOF air damped vibrating system data selected is as, main mass $m_2 = 6.0$ kg, auxiliary mass $m_1 = 0.815$ kg, auxiliary spring rate ratio $k_1 = 970$ N/M, the spring rate of the spring supporting the main mass m_2 is $k_2 = 6300$ N / M and mass ratio is $\mu = (m_2/m_1)$ is 7.36.

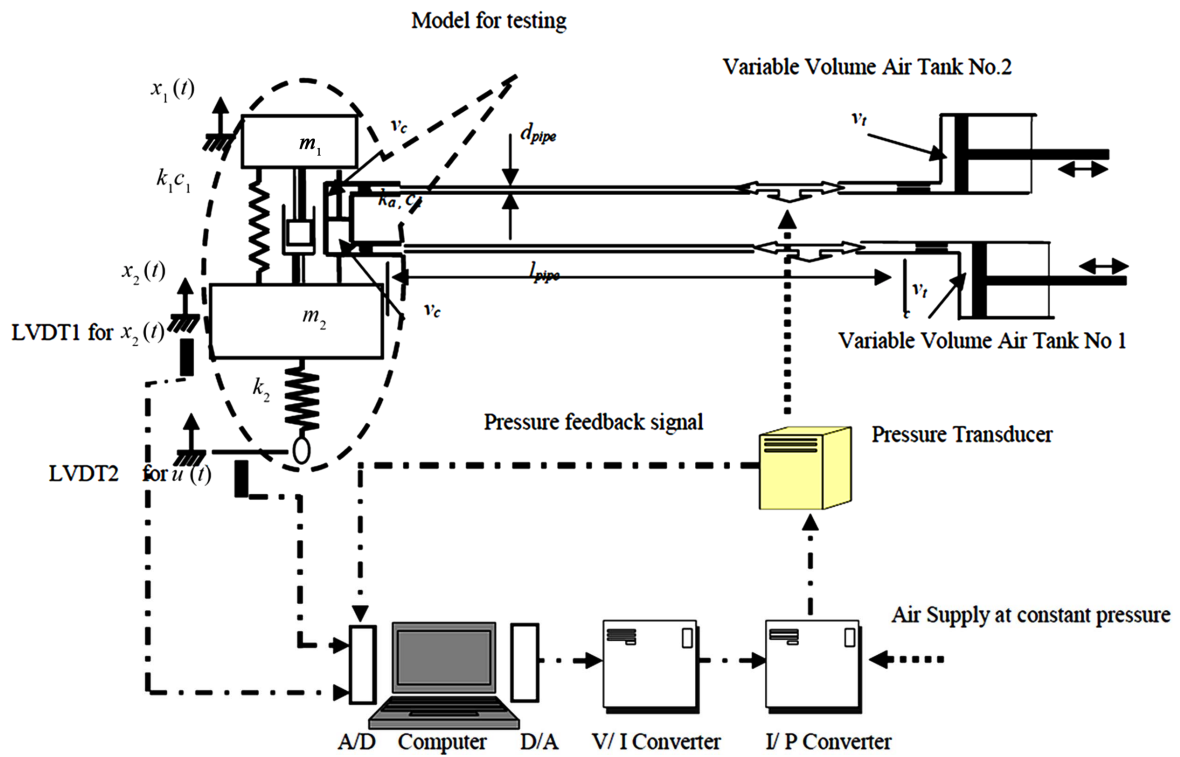


Figure 9. Experimental setup for 2DOF dynamic vibration absorber system ($\mu \gg 1$).

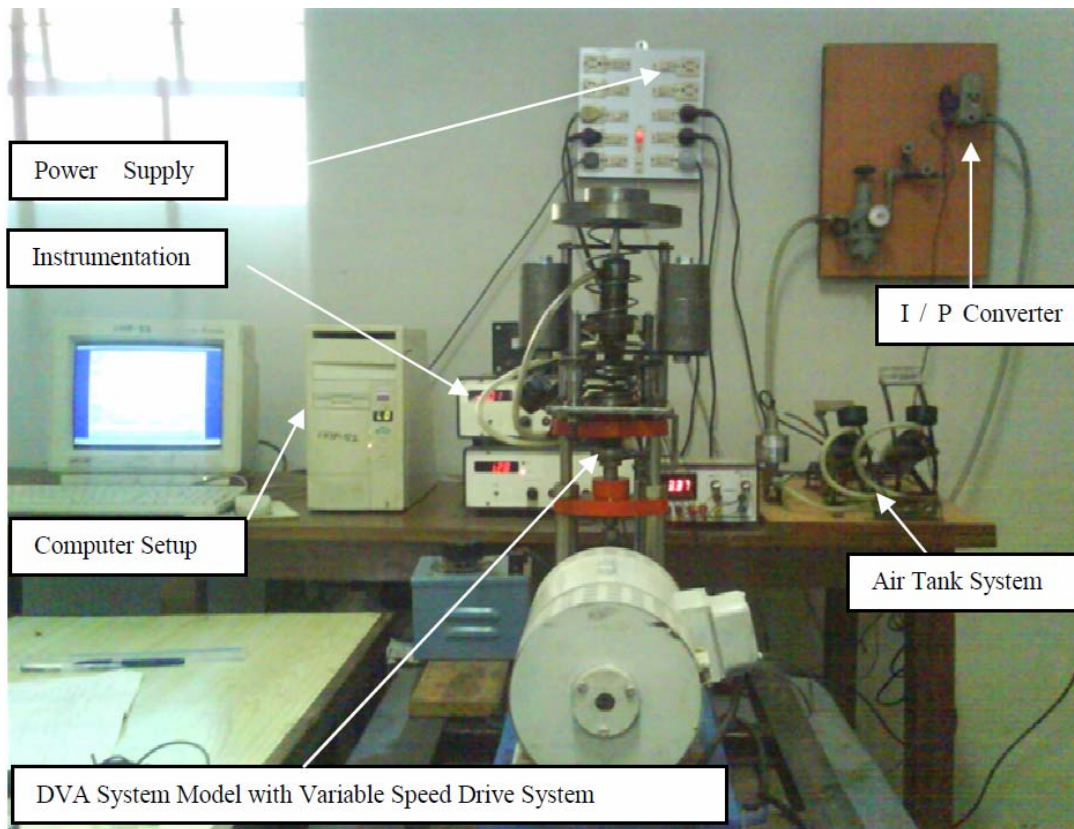


Plate 1. Experimental detup for an air damped 2DOF vibration absorber system.

5.1. Specifications of the Air Damper

Using the approach of R.D.Cavanaugh [3] for the design of air damper, following relations have been developed [4,5].

$$1) \quad k_a = (2ns^2/v_c)(pi/N_t) \tag{15}$$

$$2) \quad \zeta_a = Q_1 \left[l_{pipe} / \left\{ (pi/N_t)^{0.5} (d_{pipe})^4 \right\} \right]^{0.5}$$

$$\text{where } Q_1 = (128 s\mu_o/\pi)(v_c/2nm_1) \tag{16}$$

Using these relations, a cylinder-piston and air-tank type air damper has been developed [3]. The specifications of the developed air damper are : piston diameter $d_p = 29.85$ mm cylinder bore $d_c = 30.00$ mm., piston rod diameter $d_r = 10.00$ mm, piston length $l_p = 13.0$ mm. and height of piston bottom from the cylinder bottom $h_p = 15.00$ mm In the experimental investigation, the first step was to select the value of the air damping ratio ζ_a associated with the air spring rate ratio k to be set and the corresponding set of capillary pipe dimensions like pipe diameter d_{pipe} and pipe length l_{pipe} . The ratio (pi/N_t) , where pi is the operating air pressure and N_t is the ratio (v_r/v_c) is the basis for the selection of the air damping ratio ζ_a (also refer **Figure 10** and **Figure 11**).The parameters d_{pipe} , l_{pipe} and the ratio (pi/N_t) have been varied to change the value of damping ratio ζ_a in the system.

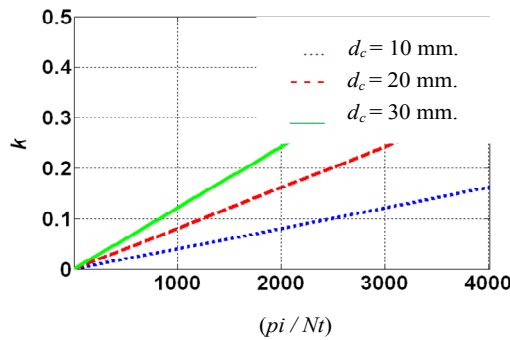


Figure 10. k vs (pi/Nt) .

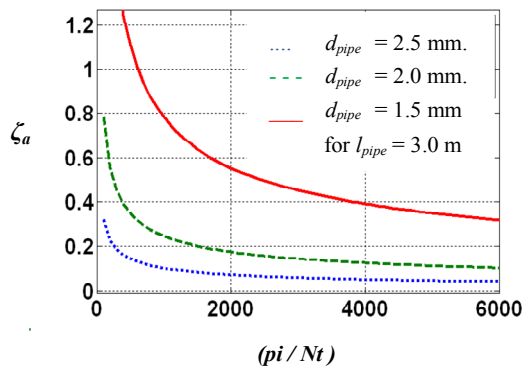


Figure 11. ζ_a vs (pi/Nt) .

5.2. Air Pressure Control

A computer interfacing system containing the closed loop air pressure control system with a set of two LVDTs to sense the main mass displacement $x_2(t)$ and base excitation $u(t)$ has been developed .The ratio (pi/N_t) plays an important role in controlling the air damping ratio ζ_a in the system. The appropriate value of the ratio (pi/N_t) , depending on the value of ζ_a desired in the system can be set by controlling the value of operating air pressure pi for a given value of the ratio $N_t = (v_r/v_c)$ or keeping the air pressure in the system at atmospheric pressure and adjusting the value of N_t by adjusting the tank volume v_t .

6. Experimental Analyses

6.1. Experimental Curves for Motion Transmissibility Mt2 vs Frequency Ratio λ

Using the experimental setup (shown in **Figure 9** and **Plate 1**) and by setting the appropriate values of the air spring rate ratio k and the air damping ratio ζ_a , the experimental plots of Mt2 vs λ have been obtained for the following cases

- 1) With $\mu = 1.5$, $\zeta_1 = 0.133$, $\zeta_2 = 0$ and without air damper.(Refer **Figure 12** and **Table 10**).
- 2) With $\mu = 1.0$, $\zeta_1 = 0.133$, $\zeta_2 = 0$ and air damper, with $k = 0.423$ and $\zeta_a = 0.1326$ (Refer **Figure 13** and **Table 11**)
- 3) With $\mu = 1.5$, $\zeta_1 = 0.133$, $\zeta_2 = 0$ and air damper, with $k = 0.423$ and $\zeta_a = 0.1326$ (Refer **Figure 14** and **Table 11**).

6.2. Experimental Curves Mt2 vs λ for Using Optimal Values of Air Damping Ratio ζ_{aopt}

Table 12 shows the theoretical and experimental peak values of motion transmissibility Mt2 at resonant frequency with the air damper set for the optimal air damping ratio ζ_{aopt} : $k = 0.1$ with $\zeta_{aopt} = 0.53$ and $k = 0.4$ with $\zeta_{aopt} = 0.68$. The experimental results have been shown in **Figure 15** and **Figure 16**.

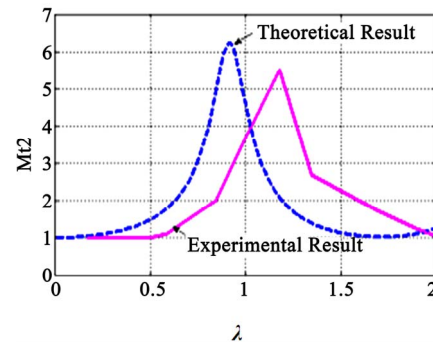


Figure 12. Mt1 vs λ for Case 6.1 (i).

Table 10. Peak values of Mt2 for Case 6.1 (i).

Peak Values of Mt2		Theoretical Results	Experimental Results
1 st peak	Mt2	6.235	5.50
	λ	0.92	1.179
Figure No.		12	

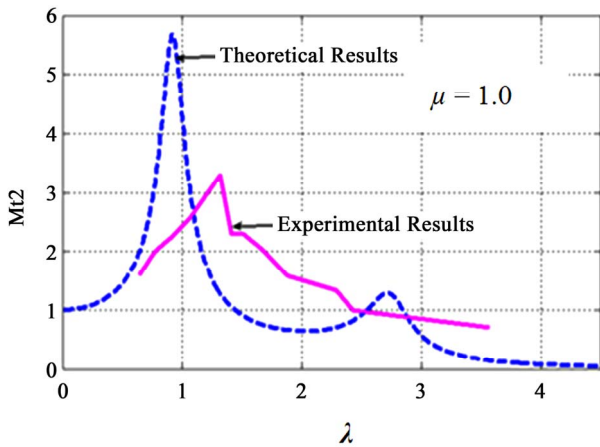


Figure 13. Mt2 vs λ for 6.1 (ii), $\mu = 1.0$, $k = 0.423$ and $\zeta_a = 0.1326$.

Table 11. Peak values of Mt2 for the Case 6.1 (ii) and for the Case 6.1 (iii) with $\zeta_1 = 0.133$, $\zeta_2 = 0.0$.

Peak Values of Mt2		$\mu = 1.0$, $k = 0.423$ and $\zeta_a = 0.1326$		$\mu = 1.5$, $k = 0.423$ and $\zeta_a = 0.1326$	
		Theoretical Values	Experimental Values	Theoretical Values	Experimental Values
1 st peak	Mt2	5.689	3.33	6.13	3.33
	λ	0.92	1.35	0.92	1.32
Figure No.		13		14	

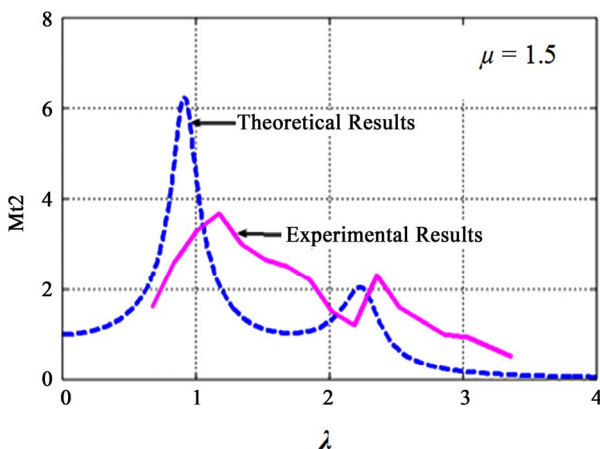


Figure 14. Mt2 vs λ for 6.1 (iii), $\mu = 1.5$, $k = 0.423$ and $\zeta_a = 0.1326$.

Table 12. Peak values of Mt2 with optimal value of optimal air damping ratio ζ_{aopt} with $\mu = 1.5$, $\zeta_1 = 0.133$, $\zeta_2 = 0.0$.

Peak Values of Mt2		Theoretical Values	Experimental Values	Theoretical Values	Experimental Values
		$k = 0.1, \zeta_{aopt} = 0.53$		$k = 0.4, \zeta_{aopt} = 0.68$	
1 st peak	Mt2	2.535	1.74	1.623	1.5
	λ	1.03	1.0	1.19	1.48
Figure No.		15		16	

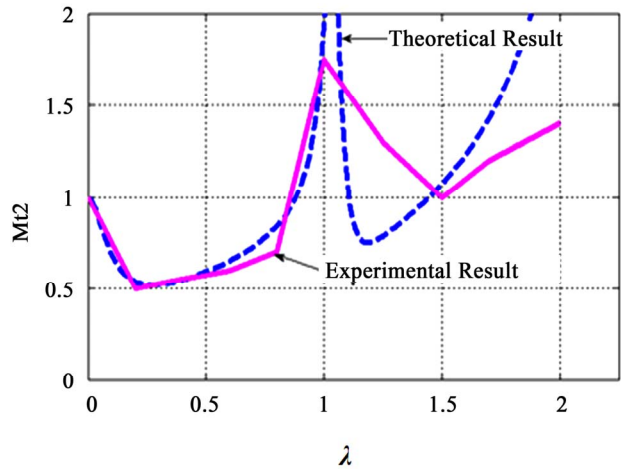


Figure 15. Mt2 vs λ . For $\mu = 1.5$, $\zeta_1 = 0.133$, $k = 0.1$, $\zeta_{aopt} = 0.53$.

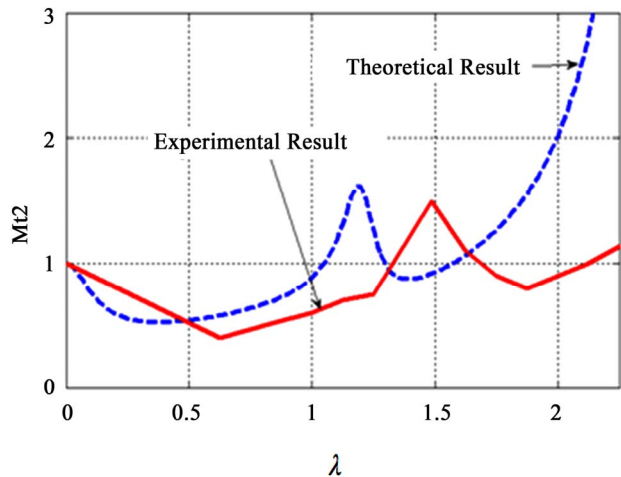


Figure 16. Mt2 vs λ . $\mu = 1.5$, $\zeta_1 = 0.133$, $k = 0.4$, $\zeta_{aopt} = 0.68$.

7. Conclusions

In this paper, the effect of mass ratio and the air damper characteristics on the resonant response of an air damped 2DOF vibrating system representing an air damped dynamic vibration absorber model have been studied with the air damper modeled as a Maxwell type. There is no substantial change in the value of Mt2 with the increase

in the value of mass ratio μ . However, with the increase in the value of the air spring rate ratio k there is a considerable increase in the value of the Mt2 at the resonant frequency where the air damper is modeled as a Maxwell type. It is seen that, with the increase in the value of the air damping ratio ζ_a there is a considerable decrease in the value of the Mt2 at the resonant frequency where the air damper is modeled as a Maxwell type. Further it is seen that as the value of the air spring rate ratio k increases, the value of the optimum value ζ_{aopt} of the air damping ratio ζ_a increases with increase in the value of motion transmissibility Mt2. It is also observed that there is a considerable reduction in the value of ζ_{aopt} with the increase in the value of the mass ratio μ , in the range $\mu = 2.5$ to $\mu = 5.0$. An experimental setup has been developed with an appropriate air pressure control system. A cylinder-piston and air-tank type air damper has been designed and developed to obtain the desired value of the air damping ratio ζ_a from the air damper. From the results of the experimental analysis shown in **Figure 13** and **Figure 14**, it is seen that the experimental peak values of Mt2 are close to the corresponding theoretical peak values of Mt2 obtained from the theoretical analysis where the air damper is modeled as a Maxwell type. From the **Figure 15** and **Figure 16**, it is seen that the theoretical and experimental values of Mt2 for $\zeta_{aopt} = 0.53$ with $k = 0.1$ and $\zeta_{aopt} = 0.68$ with $k = 0.40$ are in good agreement.

From the theoretical and experimental investigations carried out, it is seen that the addition of the air damping in the absorber system (m_l, k_l) improves substantially the motion transmissibility characteristics of the main mass

of the 2DOF dynamic vibration absorber model over a range of excitation frequencies in the region of resonance.

8. Acknowledgements

The first author Prof. R.G.Todkar acknowledges with thanks the authorities of P.V.P.Institute of Technology, Budhgaon, Dist. SANGLI (Maharashtra) INDIA 416 304 for their support and encouragement during the period of this work.

9. References

- [1] R. A. Williams, "Electronically Controlled Automotive Suspension Systems," *Computing and Control Engineering Journal*, Vol. 5, No. 3, 1994, pp. 143-148.
[doi:10.1049/cce:19940310](https://doi.org/10.1049/cce:19940310)
- [2] T. Asami and Nishihara, "Analytical and Experimental Evaluation of an Air Damped Dynamic Vibration Absorber: Design Optimizations of the Three-Element Type Model," *Transaction of the ASME*, Vol. 121, 1999, pp. 334-342.
- [3] R. D. Cavanaugh, "Hand Book of Shock and Vibration," *Air Suspension Systems and Servo-controlled Isolation Systems*, Chapter 33, pp. 1-26.
- [4] R. G. Todkar and S. G. Joshi, "Some Studies on Transmissibility Characteristics of a 2DOF Pneumatic Semi-active Suspension System", *Proceedings of International Conference on Recent Trends in Mechanical Engineering*, Ujjain Engineering College, Ujjain, 4-6 October 2007, pp. 19-28.
- [5] P. Srinivasan, "Mechanical Vibration Analysis," Tata Mc-Hill Publishing Co., New Delhi, 1990.

Nomenclature

k_1	stiffness of spring for absorber mass	d_{pipe}	inside diameter of the capillary pipe
k_2	stiffness of spring for main mass	l_{pipe}	length of the capillary pipe
m_1	absorber mass	μ_o	viscosity of air
m_2	main mass	n	index of expansion of the air
μ	mass ratio = (m_2/m_1)	k_a	stiffness of air spring
w_1	$(k_1/m_1)^{1/2}$	k	spring rate ratio = (k_a/k_1)
w_2	$(k_2/m_2)^{1/2}$	w_a	$(k_a/m_1)^{1/2}$
v	natural frequency ratio = (w_2/w_1)	c_a	coefficient of viscous damping of the air damper
ζ_1	system damping ratio for main mass system	ζ_a	damping ratio provided by the air spring
ζ_2	system damping ratio for auxikary mass system	ζ_{aopt}	optimal value of air damping ratio
w	applied frequency	$u(t)$	base excitation
λ	frequency ratio = (w/w_1)	$x_1(t)$	dynamic displacement response auxiliary mass m_1
d_p	piston diameter	$x_2(t)$	dynamic displacement response of main mass m_2
d_c	cylinder bore	Mt1	motion transmissibility of the auxiliary mass m_1
l_p	length of the piston	Mt2	motion transmissibility of the main mass m_2
h_p	height of piston from bottom of the cylinder		